LETTERS
https://doi.org/10.1038/s41563-022-01318-x

nature materials

Scalable optical manufacture of dynamic structural colour in stretchable materials

Benjamin Harvey Miller, Helen Liu and Mathias Kolle ✉

Structurally coloured materials that change their colour in response to mechanical stimuli are uniquely suited for optical sensing and visual communication[1–4]. The main barrier to their widespread adoption is a lack of manufacturing techniques that offer spatial control of the materials' nanoscale structures across macroscale areas. Here, by adapting Lippmann photography[5], we report an approach for producing large-area, structurally coloured sheets with a rich and easily controlled design space of colour patterns, spectral properties, angular scattering characteristics and responses to mechanical stimuli. Relying on just a digital projector and commercially available photosensitive elastomers, our approach is fast, scalable, affordable and relevant for a wide range of manufacturing settings. We also demonstrate prototypes for mechanosensitive healthcare materials and colorimetric strain and stress sensing for human–computer interaction and robotics.

A variety of laboratory-scale techniques currently exist for the formation of mechanoresponsive soft photonic materials[6–11]. Elastically deformable sheets and fibres of squishy opaline structures have been formed using a number of methods[12–14]. Although such materials have been produced at the macroscale[15,16], the underlying techniques do not provide spatial control over the material's optical properties and have uniformity issues at scale. Related approaches, relying on the formation of direct and inverse opals, have resulted in a few potentially viable strategies[17,18]; however, their properties are usually unsuitable for large mechanical deformations. Cellulose-based photonic laminates can be produced at scale using roll-to-roll processing, although they require the presence of water[19]; they do show impressive responsiveness to compressive stresses but are not ideal for tensile deformations, have limitations in their response time and it is difficult to achieve spatial control of the reflectance spectrum and scattering behaviour. The magnetic field-induced self-assembly of magnetic nanoparticles in a polymer matrix can be accomplished with a wide choice of material compositions, resulting in structures with tunable mechanical properties[20,21], although there are issues related to the fabrication complexity, the limited range of realizable photonic structures and trade-offs in optical performance. Block copolymer self-assembly is another technique[22,23], but it suffers from high material costs, limited scalability, and restrictions in the material composition and physical properties. Liquid crystalline elastomers have only recently emerged as a promising material platform for colour-dynamic materials and pixelated camouflage, although they still require proof of scalable manufacture and further optimization of the optical performance[24]. Direct-assembly methods have also been demonstrated, such as sequential spin coating and multilayer rolling[4] or laser interference lithography with custom photopolymers[25–27]. Although these methods offer different levels of control over the photonic architecture, they are subject to limitations around fabrication complexity, scalability, colour dynamics or equipment costs. In essence, all existing techniques are either very good at controlling the structure on the microscale but face scaling problems or are scalable but do not provide precise control over the material structure. An approach that offers both remains elusive, despite several potential high-impact applications.

Here we demonstrate a scalable method for the macroscale optical fabrication of photonic nanostructures with microscale lateral resolution in commercially available photoresponsive elastomer sheets using standard light-projection equipment. Our approach enables fine spatial control of the material's optical and mechanical properties, with access to the full visible spectrum based exclusively on structural colours, near-infrared pattern generation and a choice between specular or diffuse reflection. We unlock a rich and easily controlled material design space, previously unattainable using any competing technique, by harnessing the pioneering colour photography work of Nobel laureate Gabriel Lippmann[5]. In Lippman photography, a visual scene is inscribed into a photographic film by positioning it on a reflecting surface, which creates a pattern of standing light waves (Supplementary Video 1) that are recorded as periodic refractive index variations[28]. These refractive index variations then act as distributed Bragg reflectors, reflecting a specific part of the spectrum as a function of the structure's periodicity, which is defined by the wavelength of light in different regions of the visual scene.

We adapt Lippmann's technique by placing a sheet of commercially available elastomeric photopolymer against a reflective surface and exposing it to the image created using a standard light projector (Fig. 1; Supplementary Video 2). We focus the image on Litiholo C-RT20 holographic recording material, which is highly and reversibly stretchable and can be used without any further modification. The recording time of a structural colour pattern using these materials is between seconds and minutes, depending on the power of the light source and the size of the exposed area in which the patterns are recorded. Using high-power projection systems, we anticipate a reduction of the exposure time down to subsecond levels as the exposure time scales inversely with the light-exposure level. The photopolymer can then be bonded to silicone after a short exposure to oxygen plasma, generating structured silicone substrates that provide mechanical tunability and support (for details see Methods). These substrates also act as an optically absorbing backing layer to enhance the saturation of the reflected colours.

The design space enabled with our technique features multiple, easily controlled parameters that determine the optical and mechanical properties of the final colour-dynamic stretchable material. First, the spatial colour distribution of the projected image locally defines the period of refractive index variations that are generated in the elastomeric photopolymer, in turn determining the reflected structural colour at each point on the sheet. To demonstrate the range of available colours we created a nine-square test

Department of Mechanical Engineering, Massachusetts Institute of Technology, Cambridge, MA, USA. ✉e-mail: mkolle@mit.edu

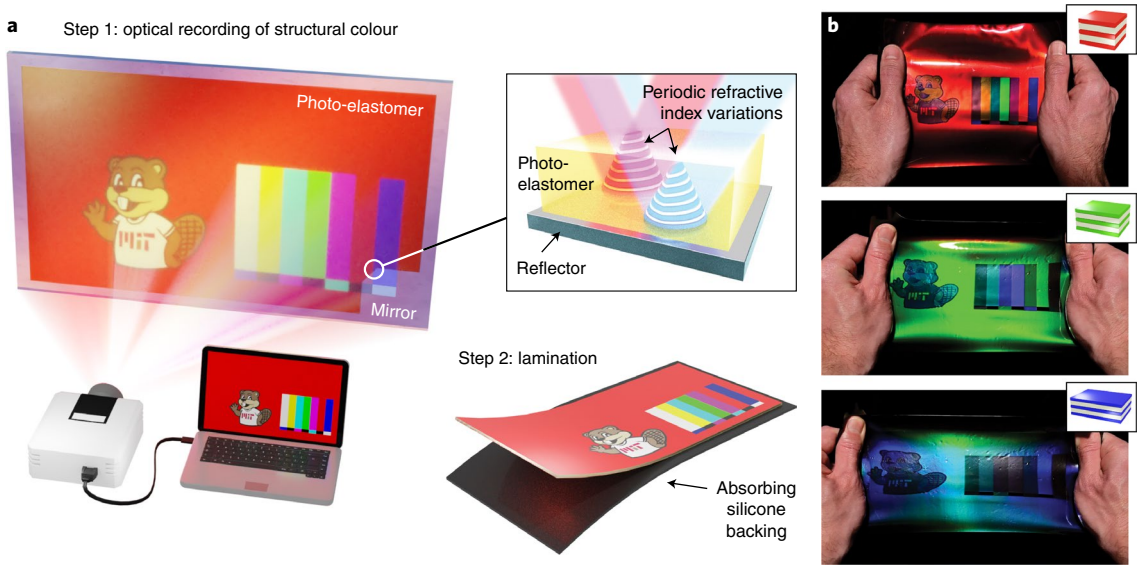

Fig. 1 | Optical manufacture of stretchable colour-changing materials at the macroscale. a, Structural colour patterns are recorded as periodic refractive index variations in the photo-elastomer via standing waves that result from exposure to a projected light pattern that reflects off the mirror backing (Supplementary Video 1). **b**, The resulting structural colour matches the spectral distribution of the exposure pattern; when the material is stretched or compressed, the periodicity of the recorded photonic structure changes, causing a predictable and reversible colour change; the shown frames are part of the recording provided in Supplementary Video 2. Image of Tim the Beaver in **a**,**b** courtesy of MIT Communication Initiatives.

image that contains the primary colours, secondary colours and shades of grey (Fig. 2a). We consistently observe a high peak reflectivity of up to 90% of incident light in the primary colour regions that match with the red, green and blue channels of the projector (Fig. 2b, top row). Akin to red–green–blue (RGB) displays, secondary colours and shades of grey (Fig. 2b, middle and bottom rows, respectively) are achieved by the superposition of individual red, green and blue spectral features, enabling the creation of structurally coloured materials of any desired hue within a single manufacturing step (Supplementary Discussion 1 and Supplementary Fig. 1). The experimentally observed reflection spectra agree closely with theoretical predictions (Supplementary Figs. 2 and 3). In contrast to light-emitting RGB displays, the peak reflectivity of the spectral features for secondary colours and shades of white are lower than the peak reflectivity of primary colours. This reduction in reflection strength for combinations of reflection bands in the material is due to the finite number of refractive index periods that can be inscribed in a photoactive polymer (Supplementary Fig. 1). This number depends on the material's thickness and the temporal coherence of the exposure illumination. Theoretical optical modelling confirms that an implementation of our approach with thicker photopolymer films results in an increase in the brightness of secondary colours and shades of white to match the brightness of primary colours (Supplementary Fig. 4). The spatial control of structural colour achievable using our technique enables the generation of materials with demanding spatio-spectral intensity distributions, such as in a flower bouquet (Fig. 2c), a motif also favoured by Gabriel Lippmann. The resolution of the structural colour patterns and the overall image area is determined by the size and resolution of the projected image (Fig. 2d). For miniaturized images of high spatial resolution, a short-focal-length lens can be added in front of the projector to achieve pixel sizes of 10 µm (Fig. 2e).

Crucially, the deformability of the elastomeric photopolymer enables a predictable, repeatable and reversible colour change in response to mechanical stimuli (Fig. 2f; Supplementary Video 3), caused by strain-induced changes to the periodicity of the photonic structures. We observe a predictable shift in the spectral reflectance peaks as a function of the applied strain (Fig. 2g; Supplementary Fig. 5) and visualize these colour trajectories by mapping each measured reflectance spectrum to a point in the Commission internationale de l'éclairage (CIE) 1931 colour space (Fig. 2h). Primary colours follow a smooth trajectory around the outside of the colour space, whereas secondary-colour regions pass closer to the central white point. An example of the variety of achievable trajectories can be seen by subjecting the flower pattern to increasing amounts of strain, with different starting colours following unique colour-space trajectories (Fig. 2h) with predictable variations in the peak reflection wavelength (Fig. 2i). The shift in the material's reflection peak centre wavelength when exposed to a lateral tensile strain is entirely predictable via mechanical modelling based on approximate knowledge of the material's Poisson's ratio (Supplementary Discussion 2). This is beneficial for the theoretical optimization of the manufacturing conditions needed to achieve any desired colour trajectory as a function of the applied strain, before production of the actual material. In the present work we have focused primarily on how mechanical deformation of the material effects the optical response; the mechanical performance of the material—a thin photopolymer laminated with a substantially thicker silicone backing—is primarily governed by the mechanical characteristics of the silicone backing. In our experiments there were no noticeable differences in deformation behaviour of material sheets with different spectral reflection bands or individual pixels in a multicoloured sheet, and all observed optical behaviour in response to mechanical deformations can be modelled reliably based on linear elasticity theory (Supplementary Fig. 5). Cyclic deformation tests confirmed that the material is durable and stable in its dynamic optical behaviour for thousands of cycles (Supplementary Discussion 3 and Supplementary Fig. 6) and that it also maintains its optical properties at elevated temperature (Supplementary Discussion 4 and Supplementary Fig. 7).

The second key parameter of our technique is the topography of the silicone backing layer, which determines the local strain caused by an externally applied tensile force. Thinner areas experience a larger strain and consequently a more pronounced colour change (Fig. 2j,k; Supplementary Video 4). We further anticipate that variation in the elastic modulus of the backing layer, akin to thickness

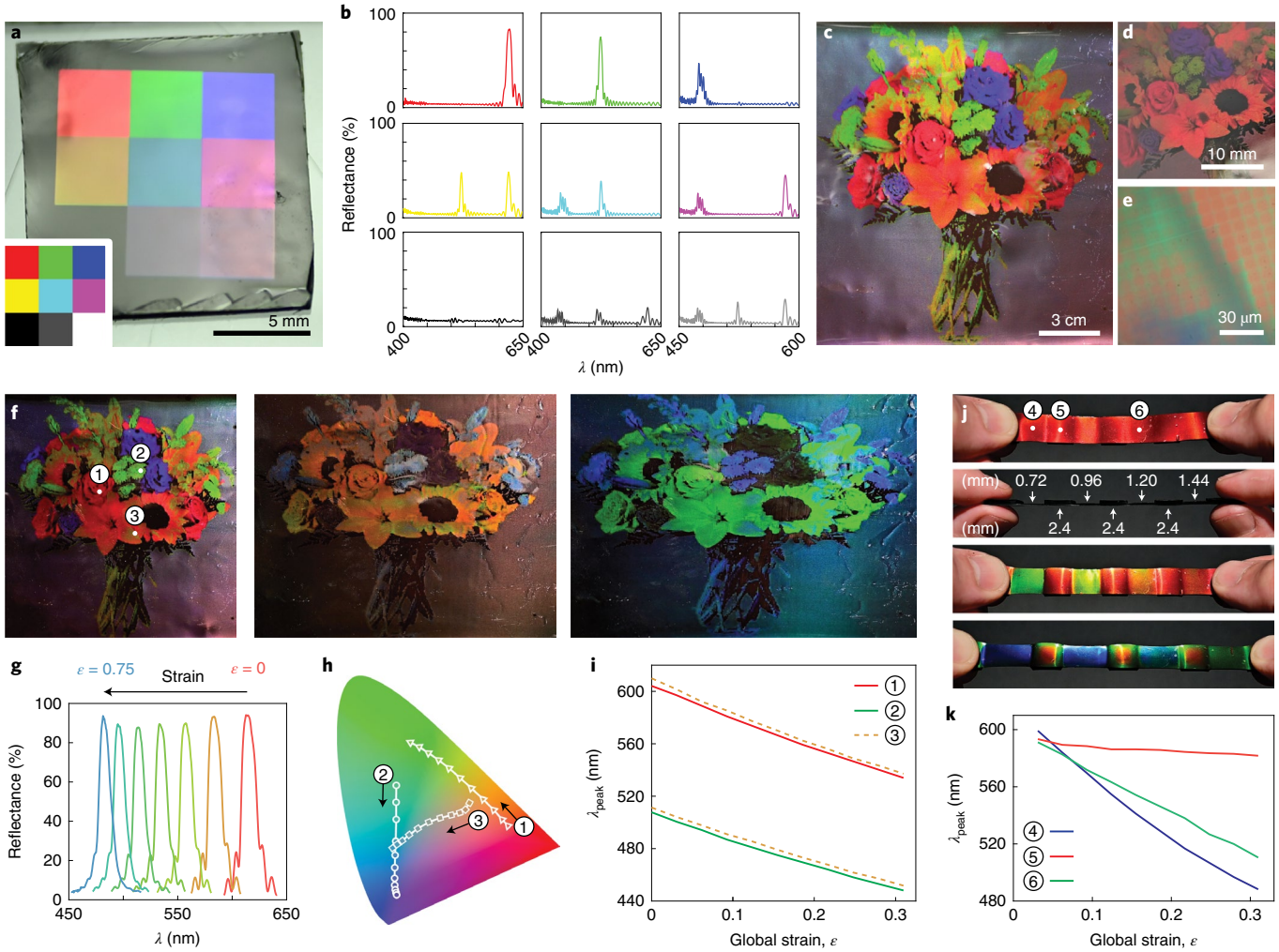

Fig. 2 | Controlling the spatial colour distribution and dynamics. a, Structural colour test sample showing primary colours (top row), secondary colours (middle row) and shades of grey (bottom row). Inset: projected digital image used to form this colour pattern. **b**, Spectra corresponding to the colours shown in **a**. **c**, A 6×8 inch structural colour analogue of a digital flower bouquet. **d**, A threefold smaller sample manufactured using the same image as in **c**. **e**, Optical micrograph of individual structural colour pixels of 10 μm size. **f**, Stretching a structural colour pattern (real-time recording in Supplementary Video 3). **g**, The structurally coloured surfaces exhibit reflectivity values above 90%. The reflection spectrum of an area with red structural colour shifts towards a lower wavelength λ as the applied strain ε is increased. **h**, Colour trajectories of the areas marked in **f** displayed in the CIE 1931 colour space. **i**, Variation of peak reflection wavelength λ_{peak} as a function of strain for the three regions marked in **f**. ① and ② mark primary colours, whereas ③ marks a secondary colour with two reflection peaks that shift in unison. **j**, Controlling the strain distribution for a given global stress through variation in the backing-layer thickness (real-time recording in Supplementary Video 4). Backing-layer thicknesses: ④, 0.72 mm; ⑤, 2.40 mm; ⑥, 1.20 mm. **k**, Variation of the peak reflection wavelength as a function of global strain for the regions marked in **j**. Credit for flower images in **c**,**d**,**f**: FTD, LLC.

variations, can serve to map a specific externally applied range of forces to a desired spatial distribution of strain, controlling the dynamic range and sensitivity.

Third, by varying the angle of incidence of light from the projector, the period of the refractive index variations can be adjusted. To demonstrate this effect, we illuminated the elastomeric photopolymer with red light at different incidence angles (Fig. 3a). The peak reflection wavelength of the resultant material increases as a function of angle, closely following theoretical predictions. We can therefore use red light to produce sheets that reflect in the near-infrared in their unstrained state, with the colour gradually shifting into the visible spectrum when strained (Fig. 3b–d; Supplementary Video 5).

Finally, the texture of the reflecting surface is another design parameter. A smooth mirror generates Bragg structures that exhibit specular structural colour. To generate a material with diffuse structural colour, which is observable over a wider range of viewing angles with reduced dependency on the illumination conditions, we use textured reflectors. Using brushed aluminium or stainless-steel plates, we transfer the reflector's angular scattering characteristics to the structurally coloured material (Fig. 3e–g; Supplementary Fig. 8). For a dynamic photonic material, this level of control over the scattering characteristics is unique to our approach.

Overall, by adapting Lippmann photography and combining it with recent advances in commercially available elastomeric photopolymers, we have developed a method for manufacturing colour-changing soft photonic materials that is scalable, flexible and accessible. The resultant materials are robust, responsive and affordable, and can be designed with a wide range of optical and mechanical properties, exhibiting a predictable and direct relationship between the applied strains and stresses and the colour change.

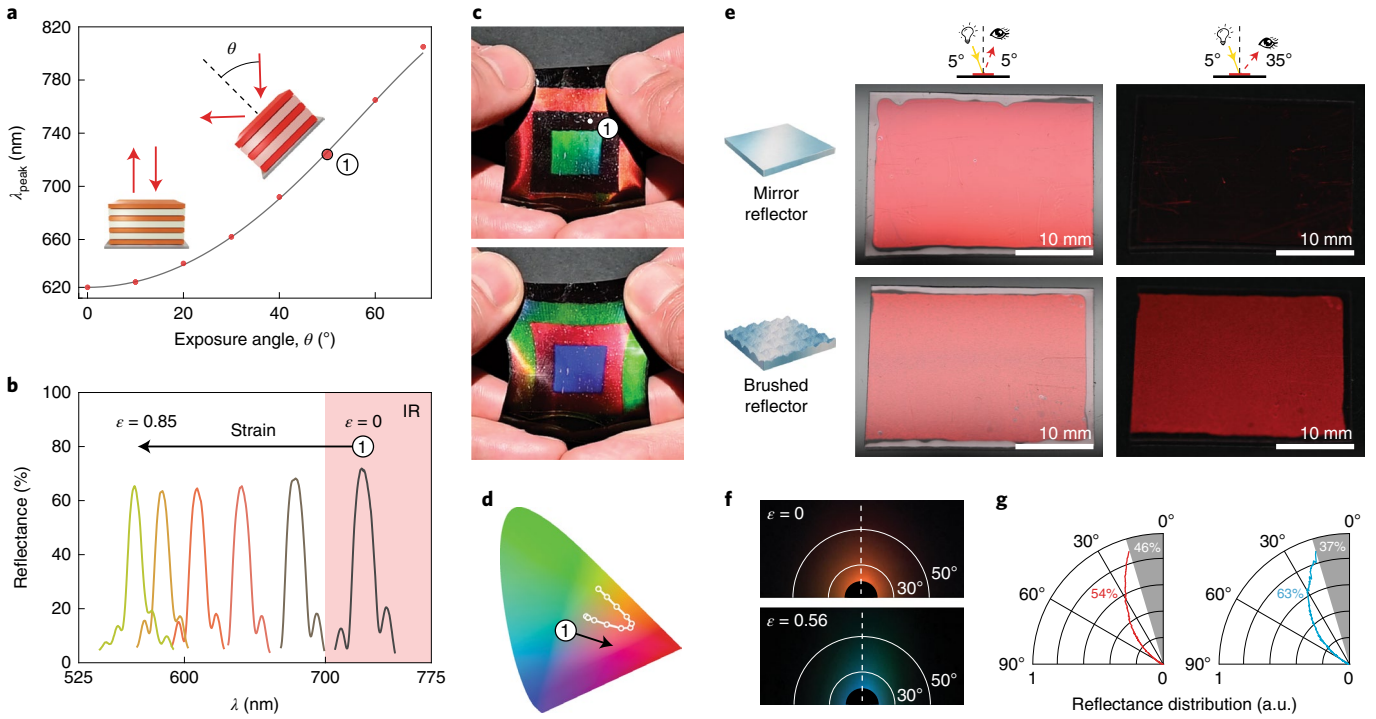

Fig. 3 | Near-infrared structural colours and tailored scattering characteristics. a, Peak reflection wavelength λ_{peak} versus exposure angle θ for an illumination wavelength of 633 nm. Exposure at increasing angles of illumination shifts the structural colour into the near-infrared region. **b**, Reflection spectrum of a sample exposed to red light at an angle of 50° (the point marked ① in **a**) and its variation with strain. IR, infrared. **c**, Sample exposed at an illumination angle of 50° using blue light (450 nm) in the centre square producing a green structural colour, red light (633 nm) in the intermediate zone (marked ①) resulting in a reflection peak in the infrared, and green light in the outer edge (532 nm), causing a red structural colour. When stretched, the dark region (①) with a reflection spectrum in the infrared region turns red (real-time recording in Supplementary Video 5). **d**, Colour trajectory of the sample region marked ① in **a**–**c** from the near-infrared to green. **e**, The light-scattering characteristics of the reflector used during exposure are transferred to the light-scattering behaviour of the resulting structurally coloured materials. A mirror backing results in a material with coloured specular reflection (top row in **e**) with the material being seen brightly only when the illumination and observation angles match. A brushed reflector is used to generate a material with a more diffuse, less angle-dependent, structural colour (bottom row in **e**). **f**, Images depicting light scattering from a structurally coloured material formed using brushed aluminium as a reflector, under relaxed (top) and strained (bottom) conditions. **g**, Polar plot showing the angular emission extracted along the white dashed lines marked in **f** for the relaxed (red) and strained (blue) material. The grey-shaded areas correspond to the blacked-out regions in **f** that mark the small-angle region in which the screen featured a hole to enable normal light exposure of the samples.

Regarding applications, providing information about mechanical forces via a colour change removes the need for sophisticated electronic or mechanical sensors, enabling observation by eye. Colorimetric indicators in elastic bandages (Fig. 4a; Supplementary Video 6) can quantify the pressure or pressure gradient being applied to a patient, a key factor for determining the optimum treatment of many medical conditions, including venous ulcers, pressure ulcers, lymphoedema and scarring[4]. Plasters (adhesive bandages) with variable-colour images (Fig. 4b) can aid with paediatric patient compliance and satisfaction. Apparel and sportswear will provide a rich canvas for stretchy colours.

By combining colour-changing sheets with simple imaging systems, such as a smartphone camera, knowledge of the quantitative relationship between strain and hue (Fig. 4c) enables more precise measurement of the mechanical forces involved. When compressive forces are applied, the observed colour change represents a map of the strain values at each location, thereby capturing the object topography (Fig. 4d–f). Knowledge of the photopolymer's elastic modulus ($E \approx 0.5$ MPa) further enables us to relate colour to pressure (Fig. 4g), which we demonstrate using the example of pushing a coin and a finger into a colour-changing sheet (Fig. 4h; Supplementary Video 7). This enables the design of compact force-sensitive devices with colour-changing sheets as the sensing element. In addition, the computational cost of analysing colour data is minimal, simply requiring the conversion of the captured image to the HSV (hue, saturation, value) colour space and applying a predefined calibration curve to the hue channel (Supplementary Discussion 5 and Supplementary Figs. 9–11), enabling high sample rates and low latency. Commonly available imaging sensors, such as those in smartphones, promise upwards of a million separate points of force data at hundreds of frames per second using our approach. The ability to obtain a real-time, high-resolution map of applied forces and deformations could be valuable in a range of areas including input devices for human–computer interactions, healthcare, motion capture, robotic locomotion and manipulation, and academic research.

Online content

Any methods, additional references, Nature Research reporting summaries, source data, extended data, supplementary information, acknowledgements, peer review information; details of author contributions and competing interests; and statements of data and code availability are available at https://doi.org/10.1038/s41563-022-01318-x.

Received: 10 August 2021; Accepted: 21 June 2022;
Published online: 1 August 2022

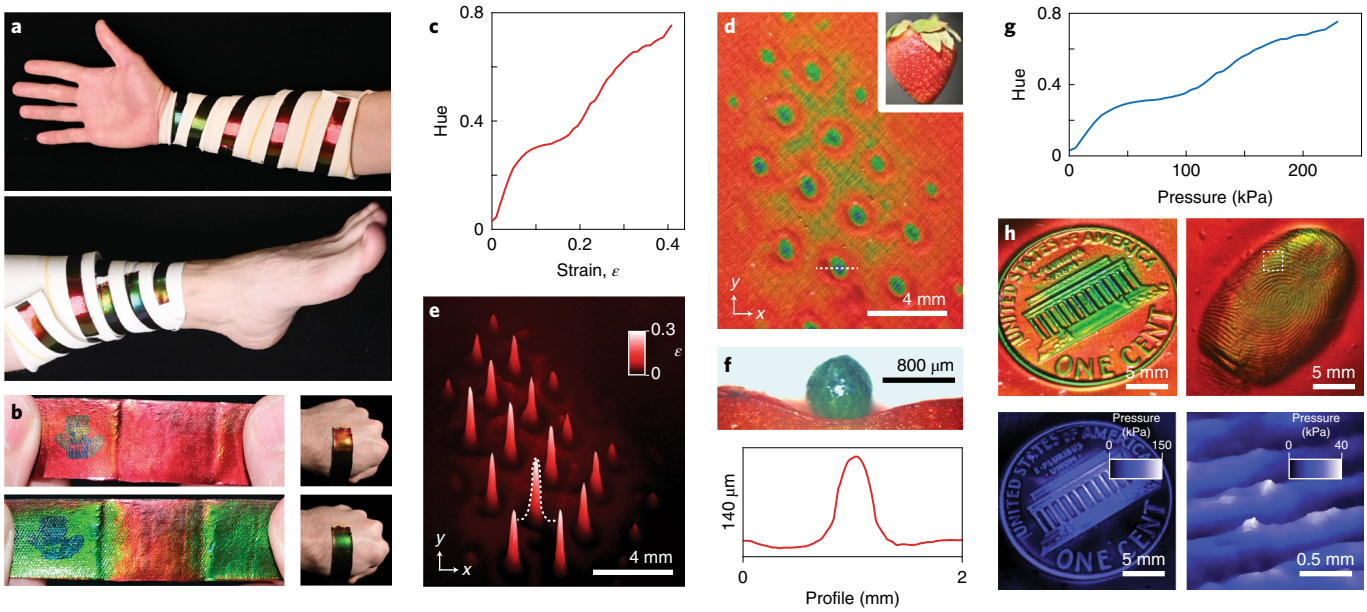

Fig. 4 | Colorimetric mechanosensing. a, Bandages equipped with colorimetric pressure indication provide information about the pressure and pressure gradient (Supplementary Video 6). **b**, Colour-changing plaster, providing an added fun factor for paediatric patients (left). When applied, the plaster mirrors any stretch in the human skin and changes colour (right). **c**, Hue versus strain, providing the basis for quantitative colorimetric strain calibration and mapping (Supplementary Figs. 9–11). **d**, Deformation-induced colour change observed when pushing a strawberry into an initially uniformly red-coloured sheet. **e**, Strawberry seed topography extracted from the colour change. **f**, Comparison between the imaged strawberry seed profile and profile deduced from the observed colour variation (sampled from the white dotted lines in Fig. 4d,e). The y-axis is the height of the detected surface in μm and the x-axis is the distance along the surface cross-section. **g**, Hue versus pressure applied to a uniformly red sheet. **h**, A one-cent coin (left) and a fingertip (right) pressed into the red sheet, with the corresponding pressure distributions (bottom) based on the quantitative relationship between pressure and hue (Supplementary Video 7), where the pressure distribution for the fingertip is shown for the area of the sheet marked by the dotted square.

References

1. Ozin, G. A. & Arsenault, A. C. P-Ink and Elast-Ink from lab to market. *Mater. Today* **11**, 44–51 (2008).
2. Yue, Y. & Gong, J. P. Tunable one-dimensional photonic crystals from soft materials. *J. Photochem. Photobiol. C* **23**, 45–67 (2015).
3. Cho, Y. et al. Elastoplastic inverse opals as power-free mechanochromic sensors for force recording. *Adv. Funct. Mater.* **25**, 6041–6049 (2015).
4. Sandt, J. D. et al. Stretchable optomechanical fiber sensors for pressure determination in compressive medical textiles. *Adv. Healthc. Mater.* **7**, 1800293 (2018).
5. Lippmann, G. La photographie des couleurs. *C. R. Hebd. Seances Acad. Sci.* **112**, 274–275 (1891).
6. Haque, Md. A., Kurokawa, T., Kamita, G., Yue, Y. & Gong, J. P. Rapid and reversible tuning of structural color of a hydrogel over the entire visible spectrum by mechanical stimulation. *Chem. Mater.* **23**, 5200–5207 (2011).
7. Zhao, Y., Xie, Z., Gu, H., Zhu, C. & Gu, Z. Bio-inspired variable structural color materials. *Chem. Soc. Rev.* **41**, 3297–3317 (2012).
8. Finlayson, C. E. & Baumberg, J. J. Polymer opals as novel photonic materials. *Polym. Int.* **62**, 1403–1407 (2013).
9. Lee, G. H. et al. Chameleon-inspired mechanochromic photonic films composed of non-close-packed colloidal arrays. *ACS Nano* **11**, 11350–11357 (2017).
10. Fu, F., Shang, L., Chen, Z., Yu, Y. & Zhao, Y. Bioinspired living structural color hydrogels. *Sci. Robot.* **3**, eaar8580 (2018).
11. Wang, Y. et al. Light-activated shape morphing and light-tracking materials using biopolymer-based programmable photonic nanostructures. *Nat. Commun.* **12**, 1651 (2021).
12. Fudouzi, H. & Sawada, T. Photonic rubber sheets with tunable color by elastic deformation. *Langmuir* **22**, 1365–1368 (2006).
13. Arsenault, A. C. et al. From colour fingerprinting to the control of photoluminescence in elastic photonic crystals. *Nat. Mater.* **5**, 179–184 (2006).
14. Ruhl, T. & Hellmann, G. P. Colloidal crystals in latex films: rubbery opals. *Macromol. Chem. Phys.* **202**, 3502–3505 (2001).
15. Finlayson, C. E. et al. Ordering in stretch-tunable polymeric opal fibers. *Opt. Express* **19**, 3144–3154 (2011).
16. Zhao, Q. et al. Large-scale ordering of nanoparticles using viscoelastic shear processing. *Nat. Commun.* **7**, 11661 (2016).
17. Kim, S. et al. Silk inverse opals. *Nat. Photonics* **6**, 818–823 (2012).
18. Phillips, K. R. et al. A colloidoscope of colloid-based porous materials and their uses. *Chem. Soc. Rev.* **45**, 281–322 (2016).
19. Liang, H.-L. et al. Roll-to-roll fabrication of touch-responsive cellulose photonic laminates. *Nat. Commun.* **9**, 4632 (2018).
20. Kim, H. et al. Structural colour printing using a magnetically tunable and lithographically fixable photonic crystal. *Nat. Photonics* **3**, 534–540 (2009).
21. Zhang, Y. et al. Super-elastic magnetic structural color hydrogels. *Small* **15**, 1902198 (2019).
22. Chan, E. P., Walish, J. J., Thomas, E. L. & Stafford, C. M. Block copolymer photonic gel for mechanochromic sensing. *Adv. Mater.* **23**, 4702–4706 (2011).
23. Kang, H. S. et al. Printable and rewritable full block copolymer structural color. *Adv. Mater.* **29**, 1700084 (2017).
24. Kim, S.-U. et al. Broadband and pixelated camouflage in inflating chiral nematic liquid crystalline elastomers. *Nat. Mater.* **21**, 41–46 (2022).
25. Naydenova, I., Jallapuram, R., Toal, V. & Martin, S. A visual indication of environmental humidity using a color changing hologram recorded in a self-developing photopolymer. *Appl. Phys. Lett.* **92**, 031109 (2008).
26. Yetisen, A. K. et al. Light-directed writing of chemically tunable narrow-band holographic sensors. *Adv. Opt. Mater.* **2**, 250–254 (2014).
27. Lee, K. M. et al. Reconfigurable reflective colors in holographically patterned liquid crystal gels. *ACS Photonics* **7**, 1978–1982 (2020).
28. Baechler, G., Latty, A., Pacholska, M., Vetterli, M. & Scholefield, A. Shedding light on 19th century spectra by analyzing Lippmann photography. *Proc. Natl Acad. Sci. USA* **118**, e2008819118 (2021).

Methods

Elastomeric photopolymer selection. There is a multitude of suitable materials available either for purchase, most commonly as holographic recording materials (Slavich PFG-03C, Litiholo C-RT20 or Bayfol HX200), or with published protocols for manufacture[29,30].

Material fabrication. Commercially available sheets of high-resolution photopolymer C-RT20 from Litiholo were chosen as the primary base material and purchased as sheets (6×8 inches), sandwiched between a glass plate and stiff plastic film (Supplementary Fig. 12a). In a darkroom, the stiff plastic film and photopolymer is peeled off the glass plate and applied to a reflective backing, photopolymer side down (Supplementary Fig. 12b,c). The photopolymer and reflector are then exposed to any desired light pattern (Supplementary Fig. 12d) originating from a desktop projector (Epson VS250) modified using three optical bandpass filters with different centre wavelength (CWL) and full-width at half-maximum (FWHM) values (that is, Thorlabs premium bandpass filters: 1, CWL = 633 nm and FWHM = 5 nm; 2, CWL = 532 nm and FWHM = 4 nm; and 3, CWL = 450 nm and FWHM = 10 nm) placed in the corresponding red, green and blue optical paths to tune the temporal coherence of the light (Supplementary Fig. 13). For a 6×8 inch sheet exposed at a distance of roughly 45 cm, the exposure time was four minutes. After exposure, darkroom conditions are no longer required. The stiff plastic film and photopolymer are peeled off the reflector and placed photopolymer side up in a plasma oven (Plasma Etch PE50XL; Supplementary Fig. 12e,f), where the film is exposed to 60 s of oxygen plasma. Once completed, the material is removed and blade-coated on the photopolymer side with a layer (roughly 150 µm) of Dowsil 700 black silicone sealant (Supplementary Fig. 12g), before being placed in an oven for 1 h at 70 °C to speed up curing. Once cured, the stiff plastic film is peeled off (Supplementary Fig. 12h,i). For other commercial holographic photopolymers, such as Bayfol HX200, this process is the same. For more traditional gelatin silver halide holographic materials there are some differences. In the case of Slavich PFG-03C, the gelatin is simply placed in contact with the reflecting backing and optically exposed as above. However, standard holographic development and bleaching steps are then required using JD-4 developer. After this, the gelatin film can simply be detached from its support. We have not tested bonding a silicone backing layer to the gelatin film. There will also be differences in the resultant optical and mechanical properties when this technique is used with different holographic recording materials.

Collecting reflectance spectra and colour data. A combined microscope (a custom-built Thorlabs 30 mm cage system with an Allied Vision Prosilica GT3300C camera and a ×50 0.5 NA objective), spectrometer (Ocean Optics Maya 2000) and strain rig (based on a Thorlabs MTS50) was built to analyse the material samples (Supplementary Fig. 14). Images and spectra were taken simultaneously at various levels of strain. The spectra were converted to points in the CIE 1931 colour space using MATLAB and the CIE colour-matching functions.

Collecting reflectance distribution data. A white screen with a pinhole in the centre was placed between the sample and the objective, such that the illuminating light passed from the objective, through the pinhole, hit the sample and was reflected back onto the screen. The screen was then imaged using a Nikon Z6 camera with a Nikon Z 50 mm *f*/1.8 lens (2 s, *f*/8, ISO 800, Flat picture control) and a two-dimensional projective transformation was applied in MATLAB. To calculate the reflectance distribution curves, the images were transformed into the $L^*a^*b^*$ colour space and a single column of the lightness channel was sampled, as shown by the white lines in Fig. 3f. The distance along the line, in pixels, was combined with knowledge of the spatial arrangement of the lens, screen and sample to calculate the corresponding reflectance angle of each pixel. To calculate the relative distribution of light between the pinhole and the screen, spectra were obtained with and without the screen in place. With the screen in place, some light is blocked from returning to the objective lens and is therefore removed from the reflectance spectrum. The blocked light is instead reflected off the screen in a well-defined region around the pinhole, enabling a conversion between the amount of light in the image and the amount of light received by the spectrometer. This conversion was then applied to the reflectance distribution image as a whole, providing an estimate of the proportion of light reflected onto the screen versus back through the pinhole.

Varying the optical pattern resolution of the material. Limited control over the optical pattern resolution of the material was achieved by moving the photopolymer closer to or further away from the projector during exposure and changing the focal length of the projector accordingly. Higher resolution samples were created by placing a 2-inch-wide 100 mm focal length plano-convex lens in front of the projector lens, followed by a Canon MP-E 65 mm macro lens focused on the photopolymer layer.

Varying the backing thickness of the material. The inverse of the shape of the desired backing layer was created as a digital model and printed in polylactic acid using a three-dimensional (3D) printer (Ender 3 Pro) to produce a mould. The mould was then treated with three coats of SuperSeal liquid sealer (Smooth-On) followed by two coats of Universal Mold Release agent (Smooth-On), as per the manufacturer's instructions. The photopolymer layer was fabricated as above; however, instead of applying a thin layer of Dowsil 700 directly it was instead squeezed into the mould and levelled. The photopolymer layer was then pressed on top, and the mould placed in an oven for one hour at 70 °C. Once cured, the Dowsil 700 was peeled from the mould, followed by peeling the stiff plastic film from the photopolymer layer.

Varying the reflecting material. Three different reflecting materials were used. The mirrored reflector was a 2×2 inch protected silver mirror (Thorlabs). Aluminium shim stock (McMaster-Carr) was used as an isotropic diffuse reflector. Stainless steel 304 with a no. 4 brush finish (McMaster-Carr) was used as an anisotropic reflector.

Bandage and plaster fabrication. The primary material fabrication method was used; however, instead of curing the silicone in the oven it was first pressed into the desired fabric while uncured, then left to cure at room temperature for 24 h. The bandage used was a SurePress high-compression bandage (ConvaTec) and the plaster was a flexible fabric adhesive bandage (Band-Aid).

Fabrication of the compression material. Although the standard material does work under compression, because of how thin the samples are they cannot capture surface features with a large range of depths. To compensate for this, a transparent silicone layer was added between the photopolymer layer and the transparent rigid support layer. To achieve this, a prefabricated sheet of material was plasma treated and placed on the outside of the bottom half of a 6 inch Petri dish, photopolymer side up, and put to one side. Three nylon spacers, whose thickness matched the desired thickness of the final material (in this case one-eighth of an inch), were placed inside the corresponding top half of the Petri dish, at the edges and forming a triangle. The Solaris liquid silicone compound (Smooth-On) was then prepared as per the manufacturer's instructions and poured into the top half of the Petri dish until the nylon spacers were fully immersed. The bottom half of the Petri dish was then gently lowered into the top half, such that the photopolymer layer was in contact with the liquid silicone. This arrangement was then left to cure for 24 h, after which the bottom half of the Petri dish was gently removed.

Fabrication of the compression device. To fabricate an integrated compression-sensing device a similar procedure was followed. A prefabricated sheet of material was plasma treated and placed on a glass plate, photopolymer side up, and put to one side. Solaris liquid silicone was then prepared as per the manufacturer's instructions and poured into the front recess of a 67 mm clear lens filter with an antireflective coating. The glass plate was then lowered onto the recess such that the photopolymer layer was in contact with the liquid silicone. This arrangement was left to cure for 24 h, after which the glass plate was gently removed. The filter was then screwed into a one-inch-long 67 mm lens hood, which was then screwed into a 3D-printed mount holding four white light-emitting diodes for illumination and an Alvium 1800 U-158c high-performance camera (Allied Vision) for imaging.

Determining the hue as a function of the compressive strain and pressure. Material samples were mounted vertically in a slide holder. They were imaged from one side using a Nikon Z6 camera with a Venus Optics Laowa 100 mm *f*/2.8 lens (1/100 s, *f*/8, ISO 2000, Flat picture control) and illuminated using an SL-60W light-emitting diode lamp (Godox). Indentation was performed with a flat indenter tip using a PT1 translation stage (Thorlabs) and UF1 force sensor (LCM Systems) with a 1.5 kg range. Images were analysed using MATLAB by converting from the RGB to HSV colour space, manually selecting a representative region and taking the mean hue value for each amount of applied strain.

Reporting summary. Further information on research design is available in the Nature Research Reporting Summary linked to this article.

Data availability

All data are available in the Letter or Supplementary information.

Code availability

All MATLAB codes used to determine the material's peak reflection wavelength and angular distribution, model its optical characteristics to compare with experimental results and predict optical performance, and the code used to convert hue into strain and stress, are available for download from https://github.com/BHMMIT/dynamic-structural-colour.' with the url 'https://github.com/BHMMIT/dynamic-structural-colour' linked.

References

29. Blyth, J., Millington, R. B., Mayes, A. G. & Lowe, C. R. A diffusion method for making silver bromide based holographic recording material. *Imaging Sci. J.* **47**, 87–91 (1999).
30. Cody, D. et al. Self-processing photopolymer materials for versatile design and fabrication of holographic sensors and interactive holograms. *Appl. Opt.* **57**, E173–E183 (2018).

Acknowledgements
B.M., H.L. and M.K. were supported by a Stepping Strong Innovator Award from the Gillian Reny Stepping Strong Center for Trauma Innovation at Brigham and Women's Hospital, the National Science Foundation through the 'Designing Materials to Revolutionize and Engineer our Future' program (DMREF-1922321), an ignition grant from the MIT Deshpande Center for Technological Innovation, a Samsung Global Research Opportunities Grant and the MIT ME MathWorks seed fund.

Author contributions
B.M. and M.K. developed the concept for the research. B.M., H.L. and M.K. conducted the experiments. B.M. and M.K. analysed the data and wrote the manuscript. All authors revised the manuscript.

Competing interests
The authors declare no competing interests.

Additional information
Supplementary information The online version contains supplementary material available at https://doi.org/10.1038/s41563-022-01318-x.

Correspondence and requests for materials should be addressed to Mathias Kolle.

Peer review information *Nature Materials* thanks Seung Hwan Ko, Yukikazu Takeoka and the other, anonymous, reviewer(s) for their contribution to the peer review of this work.

Reprints and permissions information is available at www.nature.com/reprints.

nature portfolio

Corresponding author(s): Mathias Kolle

Last updated by author(s): Mar 3, 2022

Reporting Summary

Nature Portfolio wishes to improve the reproducibility of the work that we publish. This form provides structure for consistency and transparency in reporting. For further information on Nature Portfolio policies, see our Editorial Policies and the Editorial Policy Checklist.

Statistics

For all statistical analyses, confirm that the following items are present in the figure legend, table legend, main text, or Methods section.

n/a	Confirmed
☒	☐ The exact sample size (*n*) for each experimental group/condition, given as a discrete number and unit of measurement
☒	☐ A statement on whether measurements were taken from distinct samples or whether the same sample was measured repeatedly
☒	☐ The statistical test(s) used AND whether they are one- or two-sided *Only common tests should be described solely by name; describe more complex techniques in the Methods section.*
☒	☐ A description of all covariates tested
☒	☐ A description of any assumptions or corrections, such as tests of normality and adjustment for multiple comparisons
☒	☐ A full description of the statistical parameters including central tendency (e.g. means) or other basic estimates (e.g. regression coefficient) AND variation (e.g. standard deviation) or associated estimates of uncertainty (e.g. confidence intervals)
☒	☐ For null hypothesis testing, the test statistic (e.g. *F*, *t*, *r*) with confidence intervals, effect sizes, degrees of freedom and *P* value noted *Give P values as exact values whenever suitable.*
☒	☐ For Bayesian analysis, information on the choice of priors and Markov chain Monte Carlo settings
☒	☐ For hierarchical and complex designs, identification of the appropriate level for tests and full reporting of outcomes
☒	☐ Estimates of effect sizes (e.g. Cohen's *d*, Pearson's *r*), indicating how they were calculated

Our web collection on statistics for biologists contains articles on many of the points above.

Software and code

Policy information about availability of computer code

Data collection	The images were acquired with Allied Vision's Vimba Viewer. Spectroscopic data was collected with Ocean Optics' OceanView 2.0 program and with custom Matlab 2020b code.
Data analysis	Data analysis was conducted with Matlab 2020b. The MATLAB code used to determine the material's peak reflection wavelength and angular distribution, and the code used to convert hue into strain and stress, are available for download from https://github.com/BHMMIT/dynamic-structural-colour.

For manuscripts utilizing custom algorithms or software that are central to the research but not yet described in published literature, software must be made available to editors and reviewers. We strongly encourage code deposition in a community repository (e.g. GitHub). See the Nature Portfolio guidelines for submitting code & software for further information.

Data

Policy information about availability of data

All manuscripts must include a data availability statement. This statement should provide the following information, where applicable:

- Accession codes, unique identifiers, or web links for publicly available datasets
- A description of any restrictions on data availability
- For clinical datasets or third party data, please ensure that the statement adheres to our policy

The MATLAB codes used to determine the material's peak reflection wavelength and angular distribution, the code used to convert hue into strain and stress, and the codes used for making model-based predictions about the material's optical performance are available for download from https://github.com/BHMMIT/dynamic-structural-colour.

Field-specific reporting

Please select the one below that is the best fit for your research. If you are not sure, read the appropriate sections before making your selection.

☐ Life sciences ☐ Behavioural & social sciences ☐ Ecological, evolutionary & environmental sciences

For a reference copy of the document with all sections, see nature.com/documents/nr-reporting-summary-flat.pdf

Life sciences study design

All studies must disclose on these points even when the disclosure is negative.

Sample size	*Describe how sample size was determined, detailing any statistical methods used to predetermine sample size OR if no sample-size calculation was performed, describe how sample sizes were chosen and provide a rationale for why these sample sizes are sufficient.*
Data exclusions	*Describe any data exclusions. If no data were excluded from the analyses, state so OR if data were excluded, describe the exclusions and the rationale behind them, indicating whether exclusion criteria were pre-established.*
Replication	*Describe the measures taken to verify the reproducibility of the experimental findings. If all attempts at replication were successful, confirm this OR if there are any findings that were not replicated or cannot be reproduced, note this and describe why.*
Randomization	*Describe how samples/organisms/participants were allocated into experimental groups. If allocation was not random, describe how covariates were controlled OR if this is not relevant to your study, explain why.*
Blinding	*Describe whether the investigators were blinded to group allocation during data collection and/or analysis. If blinding was not possible, describe why OR explain why blinding was not relevant to your study.*

Behavioural & social sciences study design

All studies must disclose on these points even when the disclosure is negative.

Study description	*Briefly describe the study type including whether data are quantitative, qualitative, or mixed-methods (e.g. qualitative cross-sectional, quantitative experimental, mixed-methods case study).*
Research sample	*State the research sample (e.g. Harvard university undergraduates, villagers in rural India) and provide relevant demographic information (e.g. age, sex) and indicate whether the sample is representative. Provide a rationale for the study sample chosen. For studies involving existing datasets, please describe the dataset and source.*
Sampling strategy	*Describe the sampling procedure (e.g. random, snowball, stratified, convenience). Describe the statistical methods that were used to predetermine sample size OR if no sample-size calculation was performed, describe how sample sizes were chosen and provide a rationale for why these sample sizes are sufficient. For qualitative data, please indicate whether data saturation was considered, and what criteria were used to decide that no further sampling was needed.*
Data collection	*Provide details about the data collection procedure, including the instruments or devices used to record the data (e.g. pen and paper, computer, eye tracker, video or audio equipment) whether anyone was present besides the participant(s) and the researcher, and whether the researcher was blind to experimental condition and/or the study hypothesis during data collection.*
Timing	*Indicate the start and stop dates of data collection. If there is a gap between collection periods, state the dates for each sample cohort.*
Data exclusions	*If no data were excluded from the analyses, state so OR if data were excluded, provide the exact number of exclusions and the rationale behind them, indicating whether exclusion criteria were pre-established.*
Non-participation	*State how many participants dropped out/declined participation and the reason(s) given OR provide response rate OR state that no participants dropped out/declined participation.*
Randomization	*If participants were not allocated into experimental groups, state so OR describe how participants were allocated to groups, and if allocation was not random, describe how covariates were controlled.*

Ecological, evolutionary & environmental sciences study design

All studies must disclose on these points even when the disclosure is negative.

Study description	*Briefly describe the study. For quantitative data include treatment factors and interactions, design structure (e.g. factorial, nested, hierarchical), nature and number of experimental units and replicates.*
Research sample	*Describe the research sample (e.g. a group of tagged Passer domesticus, all Stenocereus thurberi within Organ Pipe Cactus National*

Research sample	*Monument), and provide a rationale for the sample choice. When relevant, describe the organism taxa, source, sex, age range and any manipulations. State what population the sample is meant to represent when applicable. For studies involving existing datasets, describe the data and its source.*
Sampling strategy	*Note the sampling procedure. Describe the statistical methods that were used to predetermine sample size OR if no sample-size calculation was performed, describe how sample sizes were chosen and provide a rationale for why these sample sizes are sufficient.*
Data collection	*Describe the data collection procedure, including who recorded the data and how.*
Timing and spatial scale	*Indicate the start and stop dates of data collection, noting the frequency and periodicity of sampling and providing a rationale for these choices. If there is a gap between collection periods, state the dates for each sample cohort. Specify the spatial scale from which the data are taken*
Data exclusions	*If no data were excluded from the analyses, state so OR if data were excluded, describe the exclusions and the rationale behind them, indicating whether exclusion criteria were pre-established.*
Reproducibility	*Describe the measures taken to verify the reproducibility of experimental findings. For each experiment, note whether any attempts to repeat the experiment failed OR state that all attempts to repeat the experiment were successful.*
Randomization	*Describe how samples/organisms/participants were allocated into groups. If allocation was not random, describe how covariates were controlled. If this is not relevant to your study, explain why.*
Blinding	*Describe the extent of blinding used during data acquisition and analysis. If blinding was not possible, describe why OR explain why blinding was not relevant to your study.*

Did the study involve field work? ☐ Yes ☐ No

Field work, collection and transport

Field conditions	*Describe the study conditions for field work, providing relevant parameters (e.g. temperature, rainfall).*
Location	*State the location of the sampling or experiment, providing relevant parameters (e.g. latitude and longitude, elevation, water depth).*
Access & import/export	*Describe the efforts you have made to access habitats and to collect and import/export your samples in a responsible manner and in compliance with local, national and international laws, noting any permits that were obtained (give the name of the issuing authority, the date of issue, and any identifying information).*
Disturbance	*Describe any disturbance caused by the study and how it was minimized.*

Reporting for specific materials, systems and methods

We require information from authors about some types of materials, experimental systems and methods used in many studies. Here, indicate whether each material, system or method listed is relevant to your study. If you are not sure if a list item applies to your research, read the appropriate section before selecting a response.

Materials & experimental systems

n/a	Involved in the study
☒	☐ Antibodies
☒	☐ Eukaryotic cell lines
☒	☐ Palaeontology and archaeology
☒	☐ Animals and other organisms
☒	☐ Human research participants
☒	☐ Clinical data
☒	☐ Dual use research of concern

Methods

n/a	Involved in the study
☒	☐ ChIP-seq
☒	☐ Flow cytometry
☒	☐ MRI-based neuroimaging